Supporting Information

Biological activity differences between TGF-β1 and TGF-β3 correlate with differences in the rigidity and arrangement of their component monomers

Tao Huang, Seth L. Schor, and Andrew P. Hinck

Figure S1

A

	TGF-β1:TGF-β2	TGF-β1:TGF-β3	TGF-β2:TGF-β3
Human	71.4% (85.7%)	76.8% (86.6%)	79.5% (92%)
Mouse	72.3% (84.8%)	77.7% (86.6%)	78.6% (91.1%)
Chicken	64.9% (81.6%)	71.1% (82.5%)	79.5% (92.0%)
Zebrafish	56.2% (74.1%)	60.7% (75.0%)	77.7% (90.2%)

B

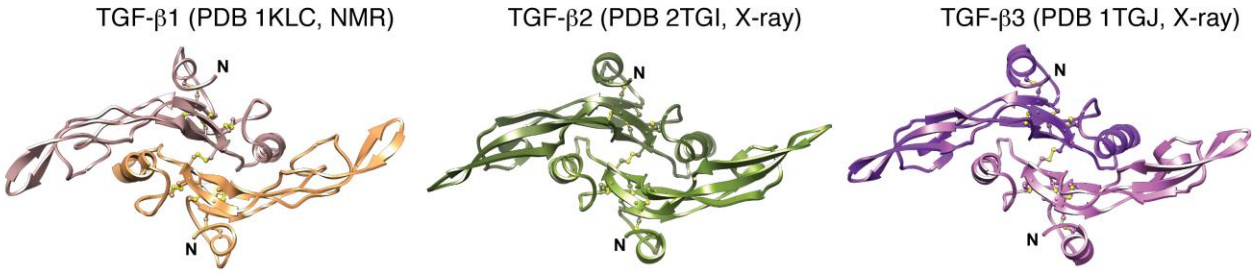

RMSD TGF-β1	0.0 Å	0.44 Å	0.42 Å
RMSD TGF-β2	0.44 Å	0.0 Å	0.31 Å
RMSD TGF-β3	0.42 Å	0.31 Å	0.0 Å

RMSDs are caclulated for all backbone N, Cα, and C atoms usign the program Superpose

Figure S1. Sequences identities and structures of the three TGF-β isoforms. A. Sequence identities and (similarities) between the mature domains of TGF-βs from different vertebrate species. B Structures of the three TGF-β isoforms. Structure of TGF-β1 was determined by NMR[1], while that of TGF-β2 and TGF-β3 were determined by crystallography[1-3]. Monomers are shaded in alternate shades of brown, green, or purple. Disulfide bonds that form the four internal disulfides in each monomer, as well as the interchain disulfide, are depicted as balls-and-sticks and are shaded yellow. Backbone RMSDs between isoforms, as calculated using the program Superpose[4], are indicated below the structures of the three isoforms.

Figure S2

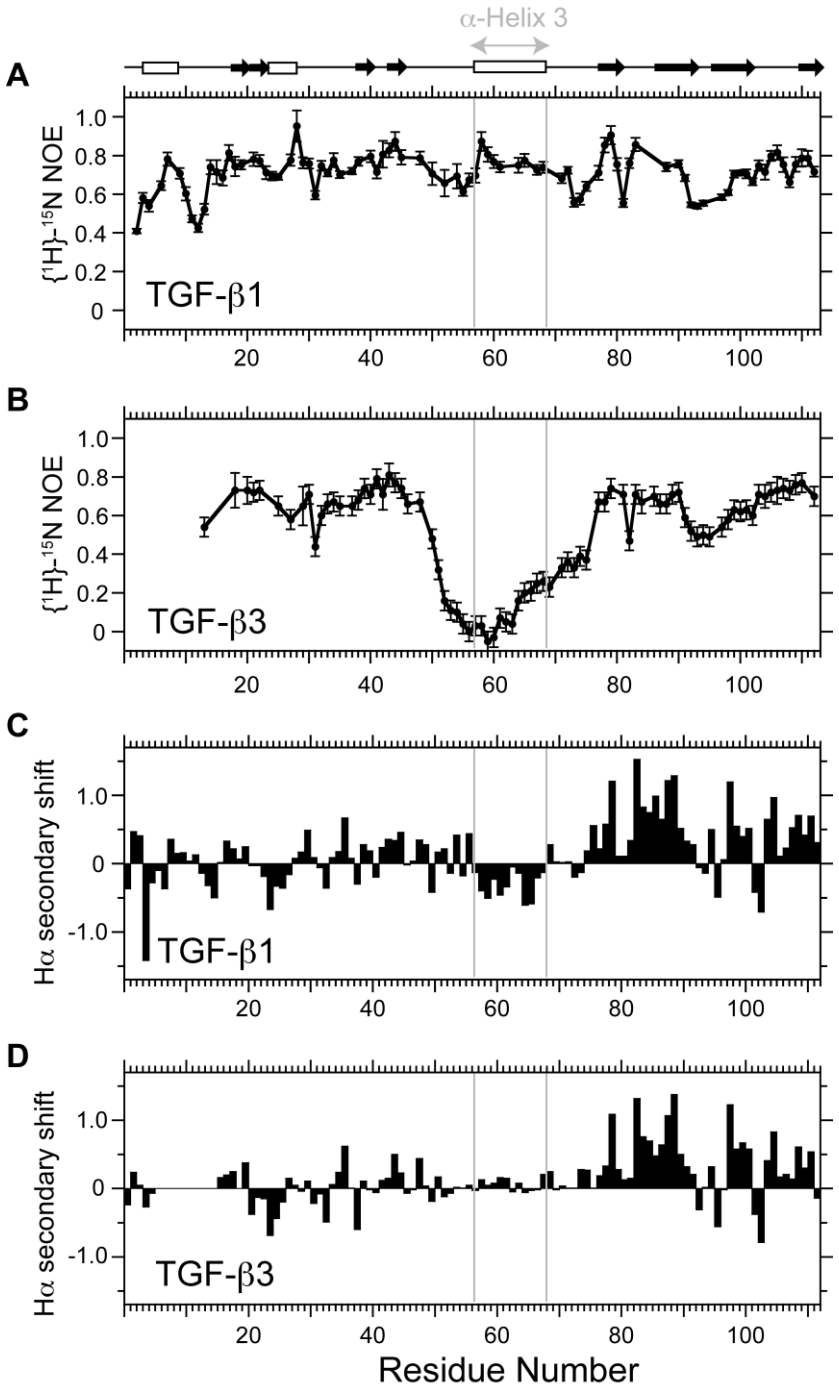

Figure S2. NMR relaxation and Hα secondary shifts of TGF-β1 and TGF-β3. A, B. $\{^1H\}$-^{15}N NOEs of TGF-β1 (A) and TGF-β3 (B). C, D. Hα secondary shifts for TGF-β1 (C) and TGF-β3 (D). $\{^1H\}$-^{15}N NOE and Hα secondary shift plots for TGF-β1 were generated from the data reported by Hinck, *et. al*[1]. $\{^1H\}$-^{15}N NOE and Hα secondary shift plots for TGF-β3 were generated from the data reported by Bocharov, et. al[5, 6].

Figure S3

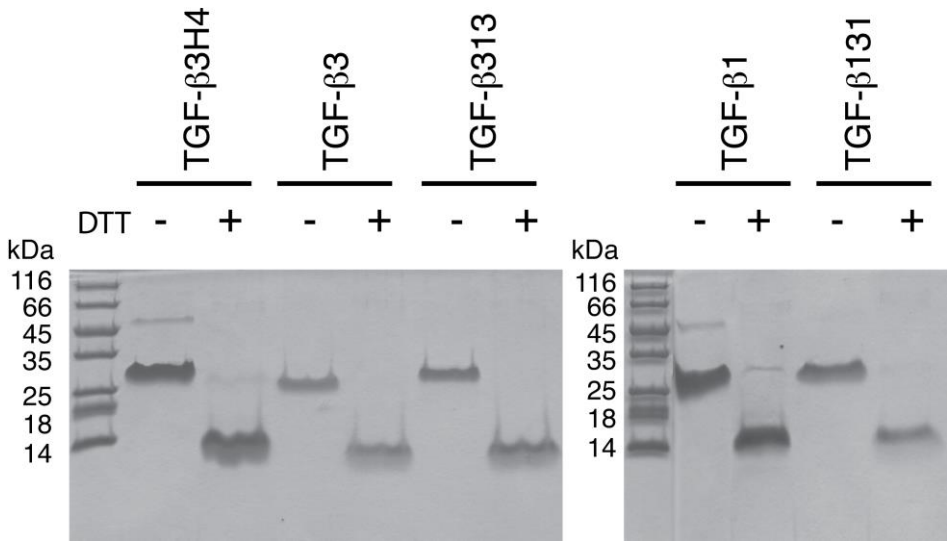

Figure S3. SDS-PAGE analysis of the purified TGF-beta homodimers. Samples were prepared with and without 100 mM DTT in the sample buffer and then run on a 12% tricine-SDS gel.

Figure S4

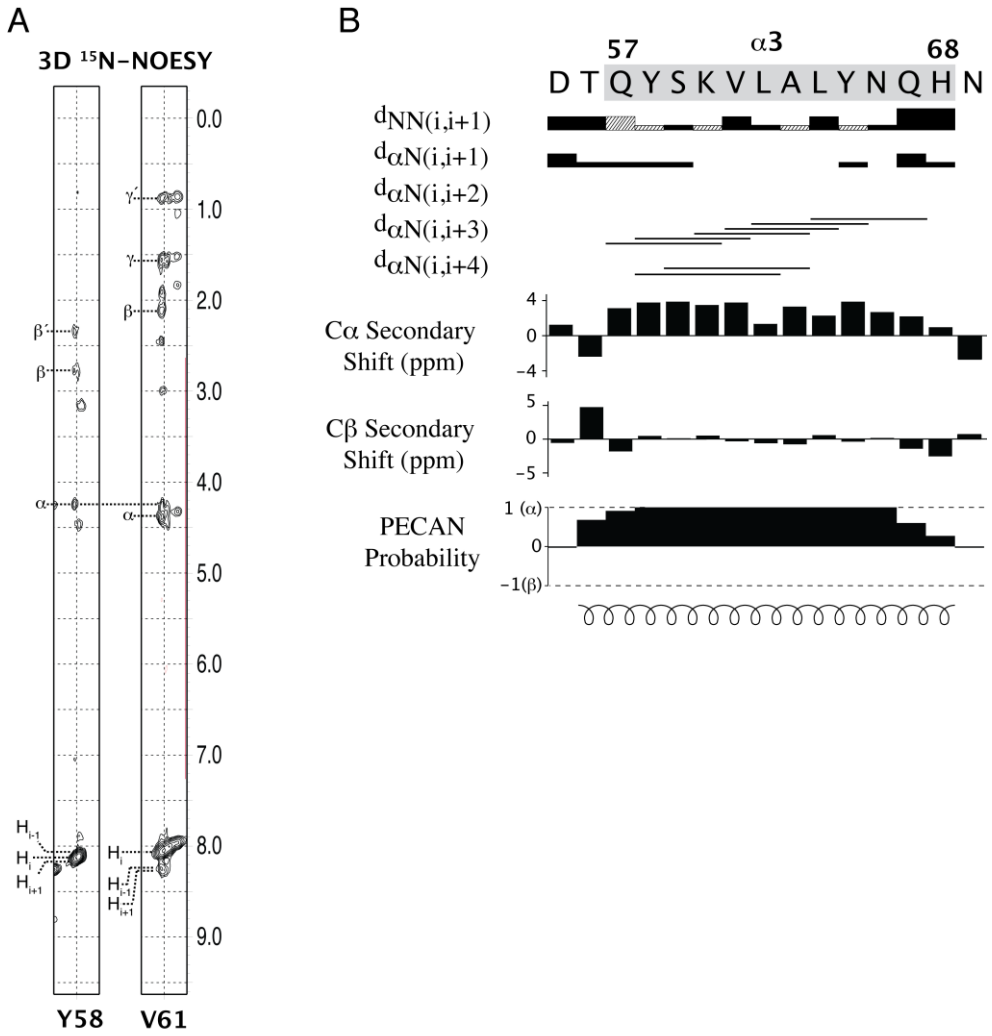

Figure S4. NMR evidence for stable α-helix between residues 57 – 68 in TGF-β313. A. Sample strips from a three-dimensional ^{15}N-edited NOESY spectrum of ^{15}N-TGF-β313 in 87% H2O, 6% dioxane-d8, and 2% methanol-d3 at pH 2.9. Spectrum was recorded at 40 °C at a proton frequency of 600 MHz. NOESY mixing time was 120 ms. B. Short- and medium-range NOEs observed in the 3D-^{15}N-edited NOESY spectrum described in A. Height of bars for d_{NN} and $d_{\alpha N}$ NOEs indicate relative intensities. Dashed bars for d_{NN} NOEs indicate it was not possible to ascertain whether an NOE was present or not due to ^{1}H resonance overlap of adjacent amides. Shown also are the Ca and Cb secondary shifts and secondary structures probabilities calculated using the program PECAN[9]. Cα and Cβ secondary shifts were calculated by subtracting the random coil Cα and Cβ chemical shifts reported by Wishart [10] from those measured.

Figure S5

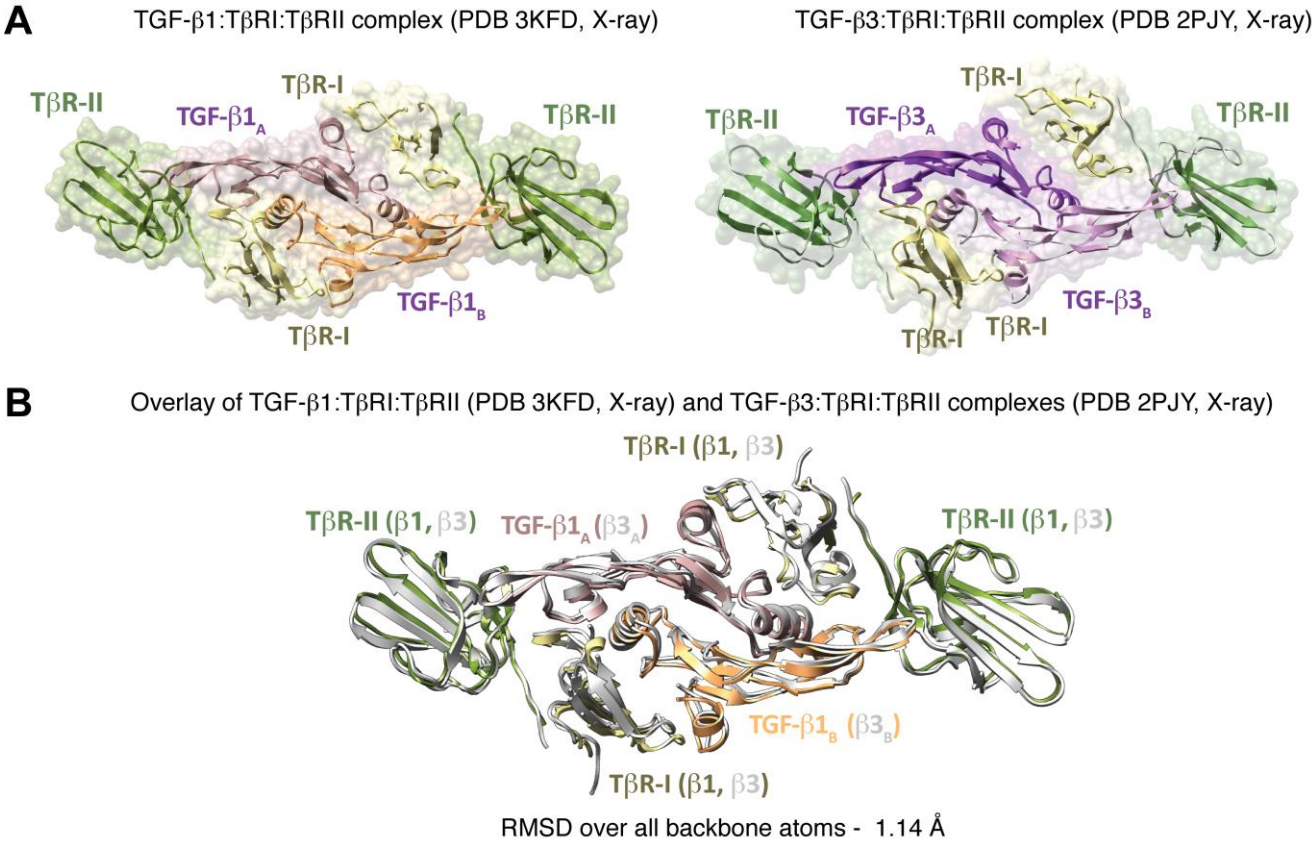

Figure S5. Structures of TGF-β1 and TGF-β3 complexed to the ectodomains of the TGF-β type I and type II receptors, TβRI and TβRII. A. Structures of the 1:2:2 TGF-β1:TβRI:TβRII (left) and 1:2:2 TGF-β3:TβRI:TβRII (right) complexes as determined by crystallography[7, 8]. B. Superposition of the structures of the 1:2:2 TGF-β1:TβRI:TβRII and 1:2:2 TGF-β3:TβRI:TβRII complexes. Structure of the TGF-β1:TβRI:TβRII complex is shaded as in panel a, while the structure of the TGF-β3:TβRI:TβRII complex is shaded gray.

Table S1 and S2

Table S1. Measured ^{15}N backbone amide T_1 and T_2 relaxation times for residues in regular regions of secondary structure in TGF-β1 and TGF-β313

Protein	Nitrogen Frequency (MHz)	T_1 (ms)	T_2 (ms)
TGF-β1	50.68	722 ± 7	72.1 ± 0.8
TGF-β313	70.95	1116 ± 66	60.0 ± 7.0

Table S2. Calculated ^{15}N backbone amide T_1 and T_2 relaxation times for residues with typical degree of backbone flexibility in structurally ordered parts of proteins (Lipari-Szabo $S^2 = 0.85$)

τ_c (ns)	Nitrogen Frequency (MHz)	T_1 (ms)	T_2 (ms)
11.7 ns	50.68 MHz	743	75.0
12.2ns	50.68 MHz	765	72.7
12.7 ns	50.68 MHz	797	69.6
11.7 ns	70.95 MHz	1180	65.4
12.2ns	70.95 MHz	1224	62.9
12.7 ns	70.95 MHz	1269	60.5

References

[1] Hinck, A. P., Archer, S. J., Qian, S. W., Roberts, A. B., Sporn, M. B., Weatherbee, J. A., Tsang, M. L., Lucas, R., Zhang, B. L., Wenker, J., and Torchia, D. A. (1996) Transforming growth factor beta 1: three-dimensional structure in solution and comparison with the X-ray structure of transforming growth factor beta 2, *Biochemistry 35*, 8517-8534.

[2] Daopin, S., Li, M., and Davies, D. R. (1993) Crystal structure of TGF-beta 2 refined at 1.8 A resolution, *Proteins 17*, 176-192.

[3] Mittl, P. R., Priestle, J. P., Cox, D. A., McMaster, G., Cerletti, N., and Grutter, M. G. (1996) The crystal structure of TGF-beta 3 and comparison to TGF-beta 2: implications for receptor binding, *Protein Sci 5*, 1261-1271.

[4] Maiti, R., Van Domselaar, G. H., Zhang, H., and Wishart, D. S. (2004) SuperPose: a simple server for sophisticated structural superposition, *Nucleic acids research 32*, W590-594.

[5] Bocharov, E. V., Blommers, M. J., Kuhla, J., Arvinte, T., Burgi, R., and Arseniev, A. S. (2000) Sequence-specific 1H and 15N assignment and secondary structure of transforming growth factor beta3, *J Biomol NMR 16*, 179-180.

[6] Bocharov, E. V., Korzhnev, D. M., Blommers, M. J., Arvinte, T., Orekhov, V. Y., Billeter, M., and Arseniev, A. S. (2002) Dynamics-modulated biological activity of transforming growth factor beta3, *The Journal of biological chemistry 277*, 46273-46279.

[7] Groppe, J., Hinck, C. S., Samavarchi-Tehrani, P., Zubieta, C., Schuermann, J. P., Taylor, A. B., Schwarz, P. M., Wrana, J. L., and Hinck, A. P. (2008) Cooperative assembly of TGF-beta superfamily signaling complexes is mediated by two disparate mechanisms and distinct modes of receptor binding, *Molecular cell 29*, 157-168.

[8] Radaev, S., Zou, Z., Huang, T., Lafer, E. M., Hinck, A. P., and Sun, P. D. (2010) Ternary complex of transforming growth factor-beta1 reveals isoform-specific ligand recognition and receptor recruitment in the superfamily, *The Journal of biological chemistry 285*, 14806-14814.

[9] Eghbalnia, H. R., Wang, L., Bahrami, A., Assadi, A., and Markley, J. L. (2005) Protein energetic conformational analysis from NMR chemical shifts (PECAN) and its use in determining secondary structural elements, *J Biomol NMR 32*, 71-81.

[10] Wishart, D. S., and Sykes, B. D. (1994) The 13C chemical-shift index: a simple method for the identification of protein secondary structure using 13C chemical-shift data, *J Biomol NMR 4*, 171-180.